Experimental Validation of the Non-Singular Terminal Sliding Mode Controller for a Process Control System

Ajit Rambhau Laware[1†], **Sneha Kuldipak Awaze**[1],
Vitthal Shrirang Bandal[2], and **Dhananjay Balu Talange**[3], Non-members

ABSTRACT

This paper presents the design of a non-singular terminal sliding mode control (NTSMC) algorithm to process a tank system which ensures high robustness, non-singularity, and finite-time convergence. The proposed control method and modified sliding manifold remove the problems associated with singularity and value complexity. The stability of the proposed strategy is proven via Lyapunov analysis, which explores the conditions for a sliding surface and error convergency in finite time to an equilibrium point or origin.

The control performance of the proposed method is comparable with classical terminal sliding mode control (TSMC) and typical continuous-time sliding mode control (SMC). The simulation and experimental results reveal the efficacy of NTSMC for estimating parameters, set-point changes from one level to another, and external disturbances. The comparison shows better process speed, settling time, rise time, non-overshoot response, and reduced chattering.

Keywords: Non-Singular Terminal Sliding Mode Control, NTSMC, Process Tank, Real-Life Experimentation

1. INTRODUCTION

Perfect liquid/water level regulation is of prime importance in processing plants for food production, chemicals, pharmaceuticals, nuclear energy, boiler drums, etc. The level of the control plant is treated as a benchmark problem due to process variability. In 95% of cases, proportional integral derivative (PID) controllers are used to regulate liquid levels. However, they do not provide a robust response due to proportional-derivative kicks, retuning of PID gains, unsatisfactory performance for time-delay systems, and lack of robustness [1, 2]. To solve the issues of robustness and stability, researchers in [3] proposed a mean-variance optimization algorithm for tuning the gains of the pitch controller in a wind turbine system using the proportional-integral controller.

A robust control strategy is needed to handle the aforementioned issues. As such, sliding mode control (SMC) is an impressive high-test control methodology for altering the system's dynamic behavior with an appropriate switching function. The existence of stability/reachability and robustness in many perturbed systems gives SMC a distinct advantage over classical controllers [4, 5]. It offers better closed-loop performance than adaptive control [6], H_2 and H_∞ control [7], and backstepping methodologies [8].

However, conventional SMC faces the problem of chattering due to the actuators potentially causing premature wear and tear. Different kinds of control strategies have been explored to alleviate the chattering effect. Levant [9] presented a second-order SMC, while Utkin *et al.* [10] used a higher-order SMC. Horch *et al.* [11] explored a super-twisting SMC for an induction motor to enhance speed, flux loops, and robustness. Through simulation, they claimed that speed and rotor flux control can be improved with the proposed strategy.

The proper choice of sliding manifold coefficients and control law parameters plays a vital role in judging a system's performance. The gain coefficient selection is a complicated, time-consuming, tedious, and challenging task. Several trials need to be conducted to address these difficulties [12].

One of the major limitations of SMC is that it stabilizes the system asymptotically during sliding mode and follows a linear sliding manifold since the output variable (controlled variable) cannot attend the desired command input in a finite time. Consequently, scholars have been motivated to improve the performance of a system during sliding mode, thereby introducing a new impressive control strategy called terminal sliding mode control (TSMC) which has non-linear sliding manifolds. If initial conditions are away from the origin, states of the system take some time to reach it [13].

To maintain motion in conventional TSMC requires an infinitely large control. Another problem with TSMC is its singularity. The authors in [14, 15] proposed a simple non-singular TSMC (NTSMC) which avoids the singularity problem completely. However, this method is

Manuscript received on January 23, 2022; revised on March 1, 2022; accepted on April 14, 2022. This paper was recommended by Associate Editor Matheepot Phattanasak.

[1]The authors are with the Department of Electrical Engineering, Dr. Vithalrao Vikhe Patil College of Engineering, Ahmednagar, India.

[2]The author is with the Government Polytechnic, Pune, India.

[3]The author is with the Department of Electrical Engineering, College of Engineering, Pune, India.

[†]Corresponding author: ajitlaware2003@gmail.com

Digital Object Identifier: 10.37936/ecti-eec.2023211.248553

only acceptable for second-order systems. The NTSMC strategy also solves the problems associated with SMC and TSMC [16]. Chiu *et al.* [17] designed a TSMC for a photovoltaic power system, while Su *et al.* [18] designed a combination of NTSMC and a disturbance observer for launch vehicles to reduce the space transportation rate in a system.

Feng *et al.* [14] studied the singularity problem of TSMC and the finite-time global stability of NTSMC for higher-order systems. The simulation results validate the superiority of the proposed method. Li and Yang [19] proposed a new TSMC strategy by focusing on the sliding mode disturbance observer for piezoelectric actuators. The uncertainties were addressed by TSMC for positioning and tracking control, while robustness was improved. Simulation was carried out to show the efficiency of the reported methodology.

Tran *et al.* [20] presented an NTSMC design for a second-order non-linear system, namely a two-link robot manipulator. The proposed method avoids the singularity problem posed by TSMC completely as well as the constraints imposed on the exponents of the mathematical function. The simulation results indicate precise tracking, finite-time convergence, and robustness in contrast to the system perturbations and unknown disturbances with reduced chattering. Cao *et al.* [21] analyzed an adaptive motion/force control method for a two-link manipulator system. After the decoupling motion and force control, a fast TSMC strategy was implemented. The simulation results show better control over earlier methods.

It is well known that conventional SMC has the serious drawback of "chattering." When the system states are not near an equilibrium point, classical SMC exhibits a slower convergence rate. It suffers from a singularity problem and complex value and also has limitations on the range of power function. To avoid these drawbacks, new TSMC designs have been proposed in [20] to improve the convergence rate.

However, the problem of singularity remains unsolved. To overcome this problem, the NTSMC strategy is proposed. However, a non-linear sliding surface restricts the power function. To solve the important issues of convergence rate, singularity, complex value, and power function restrictions, this paper proposes a modified sliding surface.

The following contributions are exploited in this research:

1. The paper verifies the effectiveness of the NTSMC method in the LTS system process. Very few researchers have applied the NTSMC strategy to process control applications for improving system performance.
2. It reports the convergence of a sliding manifold and tracking error in finite time.
3. The problem of singularity and complex value have been removed with the selection of modified sliding surface variables.
4. It avoids the reaching phase with the use of a modified NTSMC surface.
5. The proposed strategy has been compared with prevalent design methods.

This paper is structured as follows. Section 2 devises the problem formulation and motivation behind the present work. Section 3 is devoted to controller designs and stability verification of the proposed method, while Section 4 describes the real-time experimental setup. The results and discussion are covered in Section 5, while Section 6 presents the robustness analysis and concluding remarks.

2. PROBLEM FORMULATION

Consider a dynamic equation of the second-order linear system with uncertainty terms as in [22, 23]

$$\ddot{\theta}(t) = -\left(A_e \pm \Delta A_p\right)\dot{\theta}(t) - \left(B_e \pm \Delta B_p\right)\theta(t) + \left(C_e \pm \Delta C_p\right)u(t) + b_d(t) \quad (1)$$

in which $\theta(t)$ represents the controlled variable, $u(t)$ is the controlling variable, A_e, B_e and C_e are the estimated plant dynamics. ΔA_p, ΔB_p and ΔC_p are perturbations in the nominal system parameters. The term $b_d(t)$ denotes bounded disturbance while t is an independent time variable. Without perturbations, Eq. (1) can be formulated as

$$\ddot{\theta}(t) = -A_e\dot{\theta}(t) - B_e\theta(t) + C_e u(t) + b_d(t, u(t)) \quad (2)$$

where $b_d(t, u(t))$ denotes the general lumped uncertainty description satisfying $\left|b_d\right| \leq b_{dmax}$ and $b_{dmax} > 0$. Thus,

$$b_{dmax} = \pm\Delta A_p\dot{\theta}(t) \pm \Delta B_p\theta(t) \pm \Delta C_p u(t) + b_d(t) \quad (3)$$

The lower bound has been selected as zero, while the upper bound of b_{dmax} is given as [24]

$$b_{dmax} = +\Delta A_p|\dot{\theta}(t)| + \Delta B_p|\theta(t)| + \Delta C_p|u(t)| + |b_d(t)| \quad (4)$$

with the error expression as

$$e(t) = r(t) - \theta(t) \quad (5)$$

where $r(t)$ is command input signal and $\theta(t)$ denotes measured variable.

It is well known that in classical SMC, the convergence of output error does not take place at zero in a finite time. In TSMC, the linear terminal attractor is responsible for convergence speed enhancement, chattering reduction, and reaching phase elimination.

The motivation behind the present work stems from the fact that the NTSMC strategy can perform better if the problems of singularity and complex-valued functions are removed. Therefore, NTSMC-based process control methodology is implemented in this paper.

3. DESIGN OF CONTROL ALGORITHMS

3.1 Typical Sliding Mode Control

The linear sliding manifold for classical SMC is selected as in [25, 26],

$$s(t) = \dot{e}(t) + \gamma_{smc} e(t) \tag{6}$$

where γ_{smc} is a user-defined parameter and $\gamma_{smc} > 0$. It is selected in such a way that the sliding surface turns to zero within a short period.

With the derivative of Eq. (6), substituting the double derivative of Eq. (5) and considering Eq. (1), an equivalent control input $u_{eq}(t)$ is,

$$u_{eq}(t) = -(C_e)^{-1}\left[A_e\dot{\theta}(t) + B_e\theta(t) + \gamma_{smc}\dot{e}(t)\right] \tag{7}$$

while the discontinuous control input $u_{dis}(t)$ is considered as in [27]

$$u_{dis}(t) = \rho_{smc}\,\mathrm{sgn}(s(t)) \tag{8}$$

where ρ_{smc} is the design parameter responsible for the magnitude of the chattering signal.

Therefore, the formulation of the total control input $u_{smc}(t)$ is,

$$\begin{aligned} u_{smc}(t) = -(C_e)^{-1}\big[&A_e\dot{\theta}(t) + B_e\theta(t) + \gamma_{smc}\dot{e}(t) \\ &+ \rho_{smc}\,\mathrm{sgn}(s(t))\big] \end{aligned} \tag{9}$$

3.2 Basic Terminal Sliding Mode Controller

In the basic TSMC form, the sliding surface is the same as that proposed in [28],

$$s(t) = \dot{e}(t) + (\beta_{tsmc})^{\left(\frac{q}{p}\right)}\,\mathrm{sgn}(s(t)) \tag{10}$$

where a design constant β_{tsmc} is selected such that $\beta_{tsmc} > 0$, and $0 < q/p < 1$, where p, q are odd integers of $p > 0$ and $q > 0$. For $e(0) \neq 0$ and $s(t) = 0$, dynamics of the sliding manifold will converge to the origin in a finite time. The settling time of the TSMC is,

$$t_s = (\beta_{tsmc})^{-1}\left(1 - \frac{q}{p}\right)^{-1} |e(0)|^{\left(1-\frac{q}{p}\right)} \tag{11}$$

where $e(0)$ is called the terminal attractor, and the term $e(t)^{(q/p)}$ improves the finite-time convergence toward a steady-state point.

For a system indicated by Eq. (1), the total control input u_{tsmc} is,

$$\begin{aligned} u_{tsmc}(t) = -(C_e)^{-1}\big[&A_e\dot{\theta}(t) + B_e\theta(t) \\ &+ \beta_{tsmc}\left(\frac{q}{p}\right)e(t)^{\left(\frac{q-p}{p}\right)}\theta(t) \\ &+ w_{tsmc}\,\mathrm{sgn}(s(t))\big] \end{aligned} \tag{12}$$

where w_{tsmc} is the user-defined parameter and responsible for the magnitude of chattering with $w_{tsmc} > 0$.

3.3 Non-singular Terminal Sliding Mode Controller

The design of SMC requires a sliding surface as the differentiator. However, this creates a problem for a TSMC since it results in negative power. The time-derivative of the term $(\beta_{tsmc})(q/p)|e(t)|^{(q/p)-1}\,\mathrm{sgn}(s(t))\dot{s}(t)$ in Eq. (10) would produce the outcome of negative power since the condition is $(q/p) < 1$ and presents a singularity problem if $e(t) = 0$, $\dot{e}(t) \neq 0$. With these conditions, an infinite control would out-turn which is not feasible for practical applications.

Sliding surface is selected as

$$s(t) = \dot{e}(t) + \int_0^t \left[h_1(e(t))^{\alpha} + h_2 e(t) + h_3(e(t))^3 + h_4(\dot{e}(t))^{\beta}\right] \tag{13}$$

in which h_1, h_2, h_3 and h_4 are the positive coefficients, $0 < \alpha < 1$, $\beta = 2\alpha/(1+\alpha)$.

Based on the convergence rate during the sliding phase, the parameters in Eq. (13) are selected on a trial-and-error basis.

The terms in Eq. (13), $(e(t))^{\alpha}$ and $(\dot{e}(t))^{\beta}$, are defined as in [29],

$$\begin{aligned} (e(t))^{\alpha} &= (|e(t)|)^{\alpha}\,\mathrm{sgn}(s(t)) \\ (\dot{e}(t))^{\beta} &= \beta(|e(t)|)^{(\beta-1)\dot{e}(t)} \end{aligned} \tag{14}$$

where $\alpha > 0$, $\beta > 0$ with $\mathrm{sgn}(s(t)) = 1$ for $s(t) > 0$, $\mathrm{sgn}(s(t)) = -1$ for $s(t) > 0$ and $\mathrm{sgn}(s(t)) = 0$ for $s(t) = 0$.

Remark 1: The terms in Eq. (13), $h_1(e(t))^{\alpha} + h_2 e(t) + h_3(e(t))^3$ provide a faster convergence rate if $|e(t)| \gg 1$ whereas the term $h_4(\dot{e}(t))^{\beta}$ conveys finite-time convergence for $e(t) \ll 1$.

After substitution $s(t) = 0$ and $\dot{s}(t) = 0$ to ensure reachability in the sliding mode, thereby obtaining

$$\ddot{e}(t) = -\left[h_1(e(t))^{\alpha} - h_2 e(t) - h_3(e(t))^3 - h_4(\dot{e}(t))^{\beta}\right] \tag{15}$$

Remark 2: Motivation behind Eq. (13), different sliding surfaces are expressed as in [13, 14],

$$\begin{aligned} s(t) &= \dot{e}(t) + \mu[e(t)]^{\frac{q}{p}} \\ s(t) &= \dot{e}(t) + \rho e(t) + \mu[e(t)]^{\frac{q}{p}} \end{aligned} \tag{16}$$

where $\rho > 0$, $\mu > 0$, p, q are positive odd-integers satisfying the condition $1 < p/q < 2$.

If $e(t) < 0$, q/p cause the exponent $[e(t)]^{q/p} \notin \Re$ and confine the control input $[e(t)]^{(q/p)-1}\dot{e}(t)$ resulting in a singularity problem if $\dot{e}(t) \neq 0$ and $e(t) = 0$.

Another form of TSMC surface has been used in [19, 30],

$$s(t) = \dot{e}(t) + \mu|e(t)|^{\gamma}\,\mathrm{sgn}(e(t))$$

$$s(t) = \dot{e}(t) + \rho e(t) + \mu|e(t)|^{\gamma}\,\mathrm{sgn}(e(t)) \quad (17)$$

In Eq. (17), the problem of complex value is removed while the drawback of singularity remains. Therefore, the sliding manifold represented by Eq. (13) does not encounter problems with the complex-valued function and singularity.

On the simplification of Eqs. (2), (5), and (13) for $s(t) = \dot{s}(t) = 0$, an equivalent control law $u_{eq}(t)$ is,

$$u_{eq}(t) = -(C_e)^{-1}\left[\ddot{r}(t) + A_e\dot{\theta}(t) + B_e\theta(t) + h_1(e(t))^{\alpha} + h_2e(t) + h_3(e(t))^3 + h_4(\dot{e}(t))^{\beta} - b_{dmax}\right] \quad (18)$$

with the discontinuous control input stated in [27],

$$u_{dis}(t) = K_{ntsmc}\,\mathrm{sgn}(s(t)) \quad (19)$$

The total control input $u_{ntsmc}(t)$ for NTSMC is the total of Eqs. (18) and (19). To reduce the chattering effect, one can replace Eq. (19) with a tangential hyperbolic function to increase the convergence speed. The switching control input law is selected as,

$$u_{dis}(t) = K_{ntsmc}\tanh\frac{s(t)}{\Omega} \quad (20)$$

3.4 Stability Verification

Application of the control law in Eqs. (18) and (19) yields,

$$\dot{s}(t) = b_{dmax} - K_{ntsmc}\,\mathrm{sgn}(s(t)) \quad (21)$$

To evaluate the convergence property of NTSMC, Lyapunov stability analysis is used. To prove the stability, the Lyapunov candidate function is selected as proposed in [27]

$$V(t) = \frac{1}{2}s^2(t) \quad (22)$$

with the initial condition, $V(0) = 0$ and $V(t)$ is positive for $s(t) \neq 0$.

The derivative of $V(t)$ is,

$$\dot{V}(t) = s(t)\dot{s}(t) < 0 \quad (23)$$

after the substitution of Eq. (21) into Eq. (23),

$$\begin{aligned}\dot{V}(t) &= s(t)\dot{s}(t)\\ &= s(t)[-K_{ntsmc}\,\mathrm{sgn}(s(t)) + b_d(t)]\\ &= -s(t)K_{ntsmc}\frac{|s(t)|}{s(t)} + s(t)b_d(t)]\\ &= -K_{ntsmc}|s(t)| + |s(t)||b_d(t)|\\ &= -|s(t)|b_{dmax} - K_{ntsmc}\end{aligned} \quad (24)$$

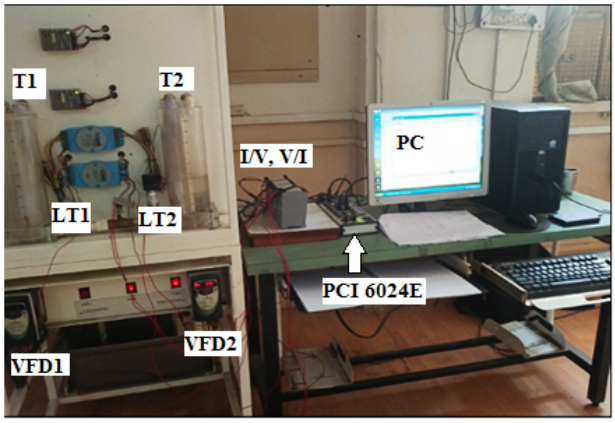

***Fig. 1**: Real-time experimental setup.*

As can be observed from Eq. (24), $\dot{V}(t) < 0$, i.e., negative semi-definite if and only if $K_{ntsmc} \geq b_{dmax}$. This indicates that the sliding surface attains zero in a finite time. Therefore, the finite-time convergence of a sliding manifold $s(t)$ is achieved if the conditions $K_{ntsmc} > 0$ and $K_{ntsmc} \geq b_{dmax}$ are satisfied.

For verification of tracking error convergence to zero during the sliding phase, the following Lyapunov function candidate is selected such that $\dot{V}_e(t) = 0$ [31, 32],

$$V_e(t) = \frac{h_1}{\alpha+1}|e(t)|^{\alpha+1} + 0.5h_2e(t)^2 + 0.25h_3e(t)^4 + 0.5\dot{e}(t)^2 \quad (25)$$

with Eq. (15) and taking the first derivative of Eq. (25), hence,

$$\dot{V}_e(t) = h_1|e(t)|^{\alpha} + h_2e(t)\dot{e}(t) + h_3e(t)^3\dot{e}(t) + \dot{e}(t)\ddot{e}(t) \quad (26)$$

Eq. (15) substituted into Eq. (26) yields,

$$\dot{V}_e(t) = -h_4\dot{e}(t)^{(\beta+1)} \leq 0 \quad (27)$$

Eq. (27) indicates the finite-time convergence of error $e(t)$ to zero since $\dot{V}_e(t)$ is a negative semi-definite function. Therefore, when $e(t) \neq 0$, the controller satisfies the Lyapunov stability condition [33], indicating good stability and robustness.

4. REAL-TIME EXPERIMENTAL SETUP

To demonstrate the practicality of SMC and its variants, the laboratory level tank system (LTS) is considered as presented in Fig. 1. Here, the objective is to maintain the liquid in the tank to the desired level. The experimental realization of the controller implementation is shown in Fig. 2.

The LTS has a pump and hand valve (V), which is 50% open. The level transmitter (LT) with an output signal of 4–20 mA DC is provided. The output of LT is converted into 0–5 V (corresponding to the 0–100% level) through a current to voltage (I/V) converter. It is then fed into the analog input (AI) of a National Instrument data card NI

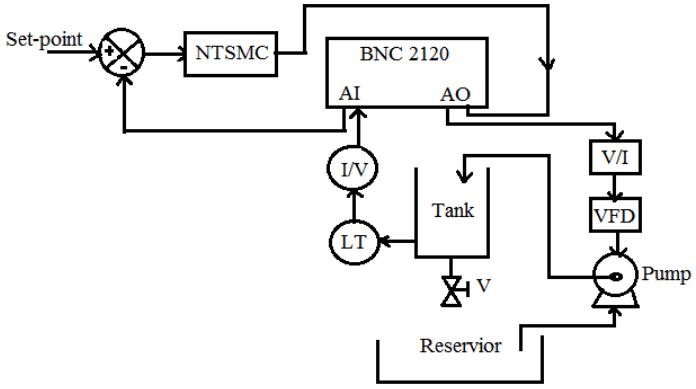

***Fig. 2**: Realization of the controller implementation.*

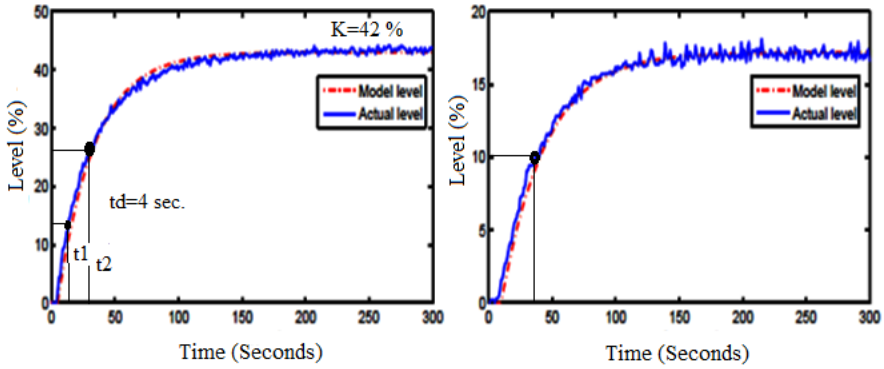

***Fig. 3**: FOPDT model parameter identification.*

PCI6024E along with a BNC connector 2120. The output of the controller (0–5 V) is applied to a variable frequency drive (VFD) through a voltage to current (V/I) converter. The VFD receives the current signal as 4–20 mA DC. The interfacing medium between the MATLAB/Simulink and LTS is the PCI6024E card. The process reaction curve method (two-point method II) is used to estimate the first-order parameters using the dead-time (FOPDT) process. From the step response curve, twice t_2 (at 63.2% of the final steady-state value) and t_1 (at 28% of the final steady-state value) are estimated, respectively. The following relations provide a FOPDT model [1].

$$\begin{aligned} K &= y_\infty \\ T &= \frac{3}{2}[t_{63} - t_{28}] \\ t_d &= (t_{63} - T) \end{aligned} \tag{28}$$

To highlight the advantages of the proposed method, parameter selection is performed on all reported controllers over many trials. The stability conditions in Eqs. (24) and (27) are referred to for parameter selection. The gains of controllers are decided from the observation of chattering signals. (Please see Section 3.3 for tuning of the control system.)

5. RESULTS AND DISCUSSION

This section explores the experimental results. The experimental response of model output and actual output are depicted in Fig. 3 following the application of 3.5 V to the pump from which the parameters of the FOPDT model are estimated. The FOPDT model is derived from the 40% level. The fitting of the model is verified for a different level (17%). From Fig. 3, one can observe that the model and actual process outputs are matched for the 40% and 17% level changes with a delay time of 4 s. An identified first-order plus dead-time model of LTS and its Taylors series approximation for dead-time are represented in Eqs. (29) and (30), respectively.

$$G_p(s) = \frac{\theta(s)}{r(s)} = \frac{0.64}{35s+1}e^{-4s} \tag{29}$$

$$G_p(s) = \frac{\theta(s)}{r(s)} = \frac{0.0049}{(s^2 + 0.2744s + 0.0061)} \tag{30}$$

Eq. (30) indicates the nominal (estimated) plant parameters as: $A_e = 0.2744$, $B_e = 0.0061$, and $C_e = 0.0049$.

The simulated and real-time performances are verified using Eq. (30) for SMC and its variants. Figs. 4(a) and 4(b) explores the NTSMC performance for nominal plant parameters with the corresponding controller output variations. The typical performance of the NTSMC

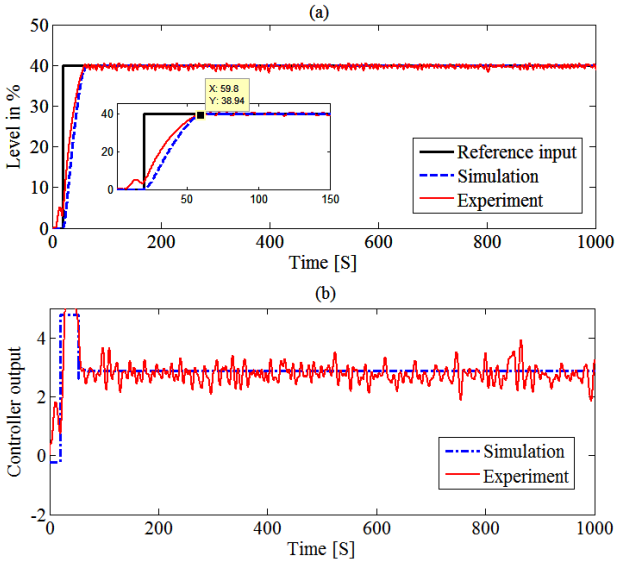

Fig. 4: NTSMC process output response, (a) estimated response and (b) controller output.

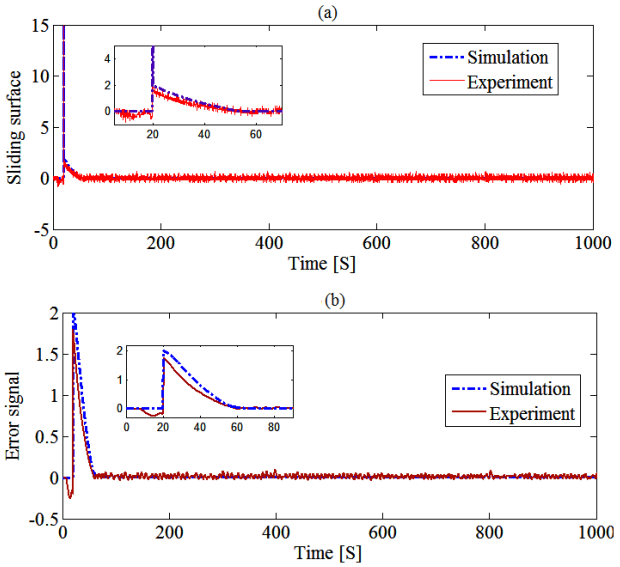

Fig. 5: Typical response of NTSMC, (a) sliding surface trend and (b) error signal variation.

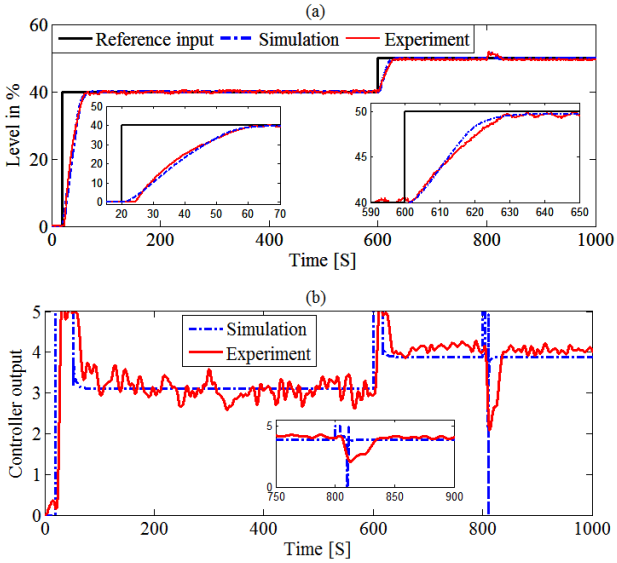

Fig. 6: NTSMC response, (a) response to reference-point changes and disturbance suppression performance and (b) associated control efforts.

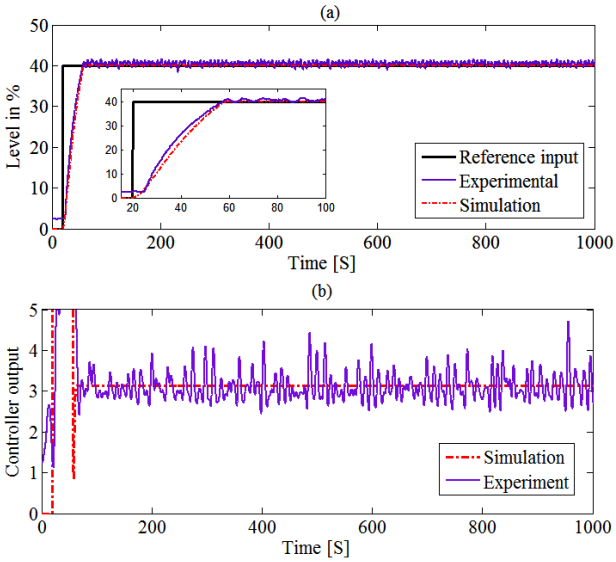

Fig. 7: TSMC output response, (a) nominal response and (b) control efforts.

strategy has been devised in Figs. 5(a) and 5(b) for sliding surface and tracking error variations.

Fig. 4(a) depicts the 0–40% level change at 58.8 s. The chattering in the controller output is ±1.064 V, as can be observed from Fig. 4(b). The sliding surface and error signal tend to reach zero at 48.23 s and 70.2 s, respectively, as shown in Fig. 5(a) and 5(b). Figs. 6(a) and 6(b) presents the performance of the NTSMC method from one level to another according to the set-point change and bounded disturbance. In all the control designs reported in this paper, at 600 s, the reference point has been changed from the 40–50% level when an external disturbance of 1.2% magnitude is applied at 800 s for a period of 10 s. The NTSMC control design method has a better disturbance rejection performance and reference-point tracking capability.

Figs. 7(a) and 7(b) explores the process and control performance of the TSMC control strategy. From Fig. 7(a), it can be observed that the percentage deviation in output is 2.15%, while the measured variable settles to the reference value at 62.2 s. The actual chattering in the controller output is ±1.734 V from the 3 V line as shown in Fig. 7(b). The sliding manifold and error convergence to zero is at 58.5 and 58.87 s, respectively, as indicated in Figs. 8(a) and 8(b). A slow response has been observed for commanding tracking and disturbance rejection with large variations in controller output as

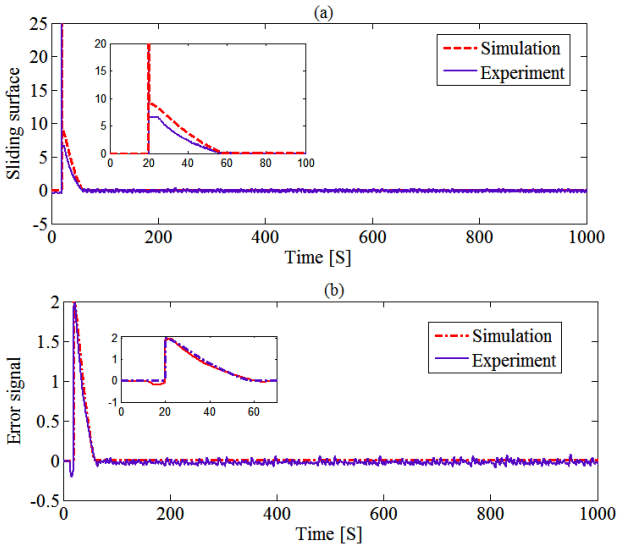

***Fig. 8**: Typical performance curve of the TSMC output response, (a) sliding surface variations and (b) error signal $e(t)$.*

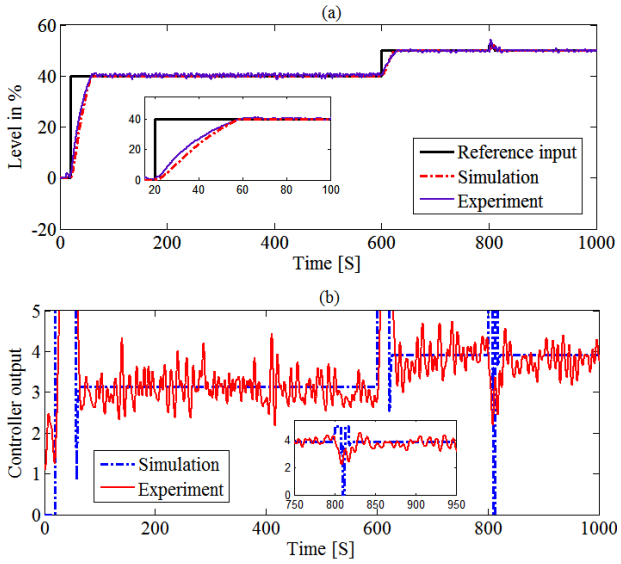

***Fig. 9**: TSMC response, (a) response to set-point change and disturbance rejection and (b) control efforts.*

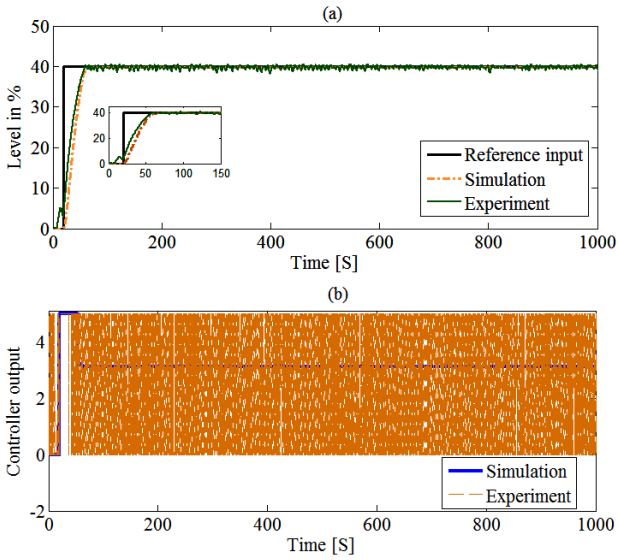

***Fig. 10**: SMC process output, (a) estimated response and (b) controller output signal.*

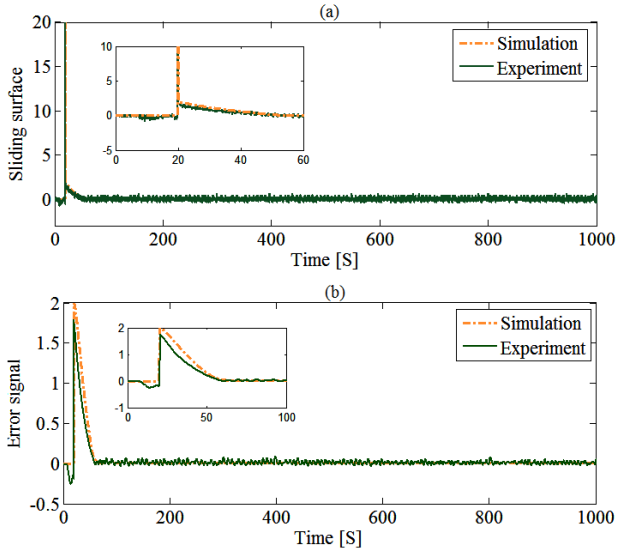

***Fig. 11**: Typical curves of the SMC, (a) sliding surface learning curves and (b) tracking error.*

analyzed in Figs. 9(a) and 9(b).

The performance of the SMC design is depicted in Fig. 10. The process variable does not settle at the reference value shown in Fig. 10(a), while the chattering is +5 V as noted in Fig. 10(b). Though the sliding surface and tracking error converges to zero earlier, the magnitude of variation is greater as indicated in Figs. 11(a) and 11(b). Reference-point tracking and disturbance suppression capability are poor, as can be observed from Figs. 12(a) and 12(b).

Summarizing the findings presented in Figs. 4–12, it can be concluded that the NTSMC provides a better performance than the TSMC and classical SMC. Table 1 shows the parameter values used in three control methods for the LTS process.

Table 2 presents a summary of the time-domain specifications, while Table 3 summarizes the error-based performance indices (IAE: Integral absolute error, ISE: Integral squared error, and MSE: Mean squared error).

Table 4 shows the chattering indices from Figs. 4(b), 5(b), and 6(b). In all three reported methods, the initial chattering signal magnitude is 5 V. From Table 4, it can be observed that chattering in the controller output is ±1.064 V which is less than other reported design methods.

As can be seen from Figs. 4–12 and Tables 2–4, the NTSMC design is more competent than other methods in terms of settling time (T_s), rise time (T_r), % overshoot (O_v), % deviation ($\%Dev.$) in output, error performance

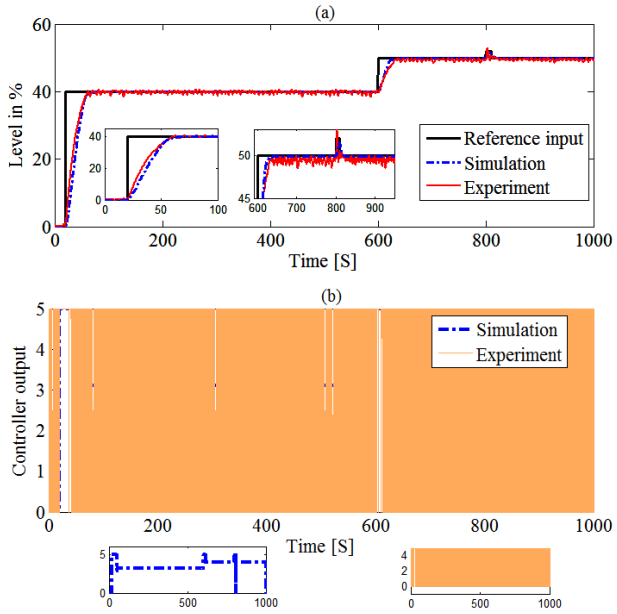

***Fig. 12**: SMC process output, (a) response to multi-level reference-point changes and disturbances and (b) corresponding control efforts.*

***Table 1**: Parameter values used in three methods for process control.*

Controller	Parameter Values
NTSMC	$\alpha = 0.1$, $\beta = 0.35$, $h_1 = 3.8$, $h_2 = 2.068$, $h_3 = 0.5$, $h_4 = 2.75$, $K_{ntsmc} = 1.5$
TSMC	$p = 3$, $q = 1$, $\beta_{tsmc} = 0.2$, $w_{tsmc} = 3.2$, $\Omega_{tsmc} = 0.035$
SMC	$\gamma_{smc} = 0.2$, $\rho_{smc} = 3.2$

***Table 2**: Summary of time-domain specifications.*

Controller Type	T_s	T_r	O_v	$\%Dev.$
NTSMC	59.8	29.2	0	1.04
TSMC	62.2	32.4	0.65	2.15
SMC	64.4	35.5	0.45	2.65

indices, and chattering. The controller output resides at 5 V for the period of 25.8 s and 38.4 s, while continuously oscillating over 1000 s for NTSMC, TSMC, and SMC strategies, respectively.

6. ROBUSTNESS ANALYSIS

To evaluate the effectiveness of reported control design methods, under the influence of parameter uncertainty, the performance of the aforementioned methods has been explored by varying the uncertainty factors. In Eq. (29), a 30% rise is considered in static gain and time constant of the process, while a 30% reduction is considered in the dead-time of the system [23, 24, 26]. With these uncertainties, the transfer function becomes,

***Table 3**: Summary of the error-based performance indices.*

Controller Type	IAE	ISE	MSE
NTSMC	79.92	49.93	0.2501
TSMC	82.52	52.12	0.301
SMC	84.25	54.07	0.437

***Table 4**: Summary of the chattering-based indices.*

Controller	Actual chattering amplitude (V)	Initial period at 5 V (s)
NTSMC	±1.064	25.8
TSMC	±1.734	38.4
SMC	+5	Oscillates between 0–5 V

$$G_p(s) = \frac{\theta(s)}{r(s)} = \frac{0.832}{45.5s + 1} e^{-2.8s} \tag{31}$$

For the realization of controllers, the Taylor series approximation of Eq. (31) is,

$$G_p(s) = \frac{\theta(s)}{r(s)} = \frac{0.00653}{(s^2 + 0.379s + 0.00785)} \tag{32}$$

Figs. 13(a)–13(f) illustrate the performance of the LTS process with 30% parameter uncertainty and disturbance. Comparing the learning curves in Figs. 6(a) and 6(b) with Figs. 13(a) and 13(b), Figs. 9(a) and 9(b) with Figs. 13(c) and 13(d), and Figs. 12(a) and 12(b) with Figs. 13(e) and 13(f), it can be concluded that under parameter uncertainty, the performance of NTSMC and TSMC are not much different, and both have a reasonably good disturbance suppression performance in comparison to the conventional SMC.

7. CONCLUSION

In this study, the non-singular terminal sliding mode control is implemented to boost the performance of a level control system. System stability is proven via the direct Lyapunov candidate function. The stability verification analyzes the finite-time and error convergence of a sliding surface. The system is modeled using the process reaction curve method II, and a first-order model with dead-time is obtained from manual mode operation of the system. The simulation and experimental results demonstrate the superiority of the NTSMC method over prevalent control strategies for processing control applications.

Invariance is achieved in opposition to perturbations and unknown disturbances. The reference-point change ability of the proposed design is better than classical control techniques. From the simulation, experimental tests, and the results exhibited in Tables 2–4, it can be observed that the control performance of the level control system is significantly enhanced with the NTSMC strategy. It

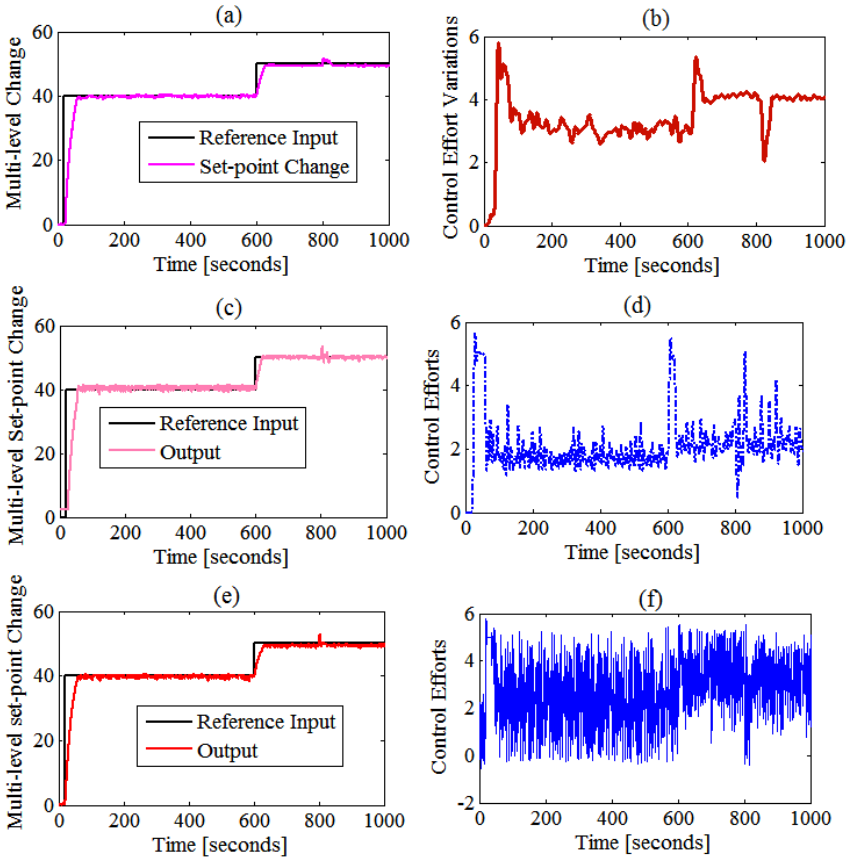

***Fig. 13**: Curve under 30% parameter uncertainty and disturbance; (a) and (b) NTSMC performance, (c) and (d) TSMC performance, and (e) and (f) SMC performance.*

shows faster convergence of the sliding surface and error signal in a finite-time interval. The NTSMC also exhibits a better performance in set-point change and external disturbance. Therefore, the proposed strategy can be adopted for industrial use to improve the performance and accuracy of a feedback control system. With the modified sliding surface selected in this article, the problems of singularity and complex value have been removed.

REFERENCES

[1] D. E. Seborg, T. F. Edgar, and D. A. Mellichamp, *Process Dynamics and Control*, 2nd ed. New Delhi, India: Wiley India, 2006.

[2] M. Huba, "Performance measures, performance limits and optimal PI control for the IPDT plant," *Journal of Process Control*, vol. 23, no. 4, pp. 500–515, Apr. 2013.

[3] S. Behera and S. Sahoo, "Design of a pitch controller for a wind turbine using hybrid mean-variance mapping optimization," *ECTI Transactions on Electrical Engineering, Electronics, and Communications*, vol. 19, no. 3, pp. 298–311, Oct. 2021.

[4] A. R. Laware, D. B. Talange, and V. S. Bandal, "Temperature control of heat exchanger using sliding mode control law," *Journal of Control & Instrumentation*, vol. 6, no. 1, pp. 14–26, 2015.

[5] A. Laware, D. Talange, and V. Bandal, "Design of predictive sliding mode controller for cascade control system," in *2016 IEEE First International Conference on Control, Measurement and Instrumentation (CMI)*, 2016, pp. 284–289.

[6] S. Sastry and M. Bodson, *Adaptive Control : Stability, Convergence, and Robustness*. New York, USA: Dover Publications, 2011.

[7] B. M. Chen, *Robust and H_∞ Control*. London, UK: Springer, 2000.

[8] M. Krstić, I. Kanellakopoulos, and P. V. Kokotović, *Nonlinear and Adaptive Control Design*. New York, USA: Wiley, 1995.

[9] A. Levant, "Sliding order and sliding accuracy in sliding mode control," *International Journal of Control*, vol. 58, no. 6, pp. 1247–1263, Dec. 1993.

[10] V. Utkin, A. Poznyak, Y. Orlov, and A. Polyakov, "Conventional and high order sliding mode control," *Journal of the Franklin Institute*, vol. 357, no. 15, pp. 10 244–10 261, Oct. 2020.

[11] M. Horch, A. Boumédiène, and L. Baghli, "Sensorless high-order sliding modes vector control for induction motor drive with a new adaptive speed observer using super-twisting strategy," *International Journal of Computer Applications in Technology*, vol. 60, no. 2, pp. 144–153, 2019.

[12] Y. B. Shtessel, I. A. Shkolnikov, and M. D. Brown, "An asymptotic second-order sliding mode control," *Asian Journal of Control*, vol. 5, no. 4, pp. 498–504, Oct. 2008.

[13] Y. Feng, F. Han, and X. Yu, "Chattering free full-order sliding-mode control," *Automatica*, vol. 50, no. 4, pp. 1310–1314, Apr. 2014.

[14] Y. Feng, X. Yu, and F. Han, "On nonsingular terminal sliding-mode control of nonlinear systems," *Automatica*, vol. 49, no. 6, pp. 1715–1722, Jun. 2013.

[15] S.-Y. Chen and F.-J. Lin, "Robust nonsingular terminal sliding-mode control for nonlinear magnetic bearing system," *IEEE Transactions on Control Systems Technology*, vol. 19, no. 3, pp. 636–643, May 2011.

[16] M. Jin, J. Lee, and K. K. Ahn, "Continuous nonsingular terminal sliding-mode control of shape memory alloy actuators using time delay estimation," *IEEE/ASME Transactions on Mechatronics*, vol. 20, no. 2, pp. 899–909, Apr. 2015.

[17] C.-S. Chiu, Y.-L. Ouyang, and C.-Y. Ku, "Terminal sliding mode control for maximum power point tracking of photovoltaic power generation systems," *Solar Energy*, vol. 86, no. 10, pp. 2986–2995, Oct. 2012.

[18] R. Su, Q. Zong, B. Tian, and M. You, "Comprehensive design of disturbance observer and nonsingular terminal sliding mode control for reusable launch vehicles," *IET Control Theory & Applications*, vol. 9, no. 12, pp. 1821–1830, Aug. 2015.

[19] J. Li and L. Yang, "Finite-time terminal sliding mode tracking control for piezoelectric actuators," *Abstract and Applied Analysis*, vol. 2014, 2014, Art. no. 760937.

[20] M.-D. Tran and H.-J. Kang, "Nonsingular terminal sliding mode control of uncertain second-order nonlinear systems," *Mathematical Problems in Engineering*, vol. 2015, 2015, Art. no. 181737.

[21] Q. Cao, S. Li, and D. Zhao, "Adaptive motion/force control of constrained manipulators using a new fast terminal sliding mode," *International Journal of Computer Applications in Technology*, vol. 49, no. 2, pp. 150–156, 2014.

[22] V. I. Utkin, *Sliding Modes in Control and Optimization*. Berlin, Germany: Springer-Verlag, 1992.

[23] A. Laware, D. Talange, and V. Bandal, "Evolutionary optimization of sliding mode controller for level control system," *ISA Transactions*, vol. 83, pp. 199–213, Dec. 2018.

[24] B. J. Parvat and B. M. Patre, "Fast terminal sliding mode controller for square multivariable processes with experimental application," *International Journal of Dynamics and Control*, vol. 5, pp. 1139–1146, Dec. 2017.

[25] H. K. Khalil, *Nonlinear Systems*, 3rd ed. Upper Saddle River, New Jersey, USA: Prentice Hall, 2002.

[26] M. G. Ghogare, S. L. Patil, and C. Y. Patil, "Experimental validation of optimized fast terminal sliding mode control for level system," *ISA Transactions*, vol. 126, pp. 486–497, Jul. 2022.

[27] J.-J. E. Slotine and W. Li, *Applied Nonlinear Control*. Upper Saddle River, New Jersey, USA: Prentice Hall, 1991.

[28] A. T. Vo and H.-J. Kang, "An adaptive terminal sliding mode control for robot manipulators with non-singular terminal sliding surface variables," *IEEE Access*, vol. 7, pp. 8701–8712, 2019.

[29] S. T. Venkataraman and S. Gulati, "Control of nonlinear systems using terminal sliding modes," in *1992 American Control Conference*, 1992, pp. 891–893.

[30] A. Polyakov and L. Fridman, "Stability notions and Lyapunov functions for sliding mode control systems," *Journal of the Franklin Institute*, vol. 351, no. 4, pp. 1831–1865, Apr. 2014.

[31] J. A. Souza, "Complete Lyapunov functions of control systems," *Systems & Control Letters*, vol. 61, no. 2, pp. 322–326, Feb. 2012.

[32] S. Ding, L. Liu, and J. H. Park, "A novel adaptive nonsingular terminal sliding mode controller design and its application to active front steering system," *International Journal of Robust and Nonlinear Control*, vol. 29, no. 12, pp. 4250–4269, Aug. 2019.

[33] J. Mendoza-Avila, D. Efimov, R. Ushirobira, and J. A. Moreno, "Numerical design of Lyapunov functions for a class of homogeneous discontinuous systems," *International Journal of Robust and Nonlinear Control*, vol. 31, no. 9, pp. 3708–3729, Jun. 2021.

Ajit Rambhau Laware received his B.E. and M.E. degrees in Instrumentation and Control Engineering from North Maharashtra University, Jalgaon and Pune University, Pune, India in 2000 and 2007 respectively. He completed his Ph.D. in Electrical Engineering from College of Engineering, Pune (COEP) in 2020. Currently, he is a Professor in the Department of Electrical Engineering at Dr. Vithalrao Vikhe Patil College of Engineering, Ahmednagar, India. His main research interest includes Process Control Systems, Optimization of Process Plant and Sliding Mode Control. He is a member of ISTE and ISOI.

Sneha Kuldipak Awaze received her B.E. and M.Tech. degrees in Electrical Engineering from Government College of Engineering, Chandrapur, India and Government College of Engineering, Amravati, India in 2008 and 2011 respectively. Currently, she is an assistant professor in the Department of Electrical Engineering at Dr. Vithalrao Vikhe Patil College of Engineering, Ahmednagar, India. Her main research interest includes Power Systems and Optimization. She is a member of ISTE.

Vitthal Shrirang Bandal received his B.E. and M.E. degrees in Electrical Engineering from Government College of Engineering, Karad, India in 1989 and 1995 respectively. He received the Ph.D. degree in System and Control Engineering from IIT Bombay, India in 2006. Currently, he is a Principal at Government Polytechnic, Pune, India. He has published about 100 referred journal and conference papers. His research interest covers Modeling of Dynamical Systems, Robust Control of Large Scale Systems, Power System stabilizer and Sliding Mode Control. He received research grants from AICTE, DST, BARC and BRNS. He is a member of IEEE, ISTE and IET.

Dhananjay Balu Talange received his B.E. and M.E. degrees in Electrical Engineering from the Walchand Engineering College, Sangali, India and Victoria Jubilee Technical Institute, Matunga, Bombay, India, in 1981 and 1983 respectively. He received the Ph.D. degree in System and Control Engineering from IIT Bombay, India in 2005. Currently, he is a Professor and Head of Electrical Engineering Department at College of Engineering, Pune, India. He has published about 100 referred journal and conference papers and 12 books. He has filed and published 4 patents. His research interest covers Nuclear Engineering, Robust Control, Process Plant Control. He received research grants from AICTE, DST, BARC and BRNS. He is a member of IEEE, ISTE and IET.